Chinese Chemical Letters 37 (2026) 111426

Contents lists available at ScienceDirect

Chinese Chemical Letters

journal homepage: www.elsevier.com/locate/cclet

Construction of donor-acceptor supramolecular organic framework with enhanced superoxide anion radical generation for photocatalytic synthesis of benzimidazole

Xianya Yao[a], Ning Han[b,*], Hui Liu[a], Lingbao Xing[a,*]

[a] School of Chemistry and Chemical Engineering, Shandong University of Technology, Zibo 255000, China
[b] Department of Electrical and Computer Engineering, University of Toronto, Toronto, ON M5S 1A4, Canada

ARTICLE INFO

Article history:
Received 21 February 2025
Revised 24 May 2025
Accepted 6 June 2025
Available online 7 June 2025

Keywords:
Supramolecular organic framework
Donor-acceptor
Superoxide anion radicals
Photocatalysis

ABSTRACT

The fabrication of three-component supramolecular organic frameworks (SOFs) is a considerable difficulty owing to the intricate noncovalent interactions and the constraints of current synthesis techniques. In this study, we designed and synthesized two photosensitive modules: a naphthalene-modified triphenylamine derivative (NA-TPA) as the donor unit, and a trimethylated viologen-modified triphenylamine (MV-TPA) as the acceptor unit. These modules can self-assemble into a novel two-dimensional SOF *via* encapsulation-enhanced donor-acceptor interactions with cucurbit[8]uril (CB[8]) in the aqueous solution. The resulting donor-acceptor SOF forms stable two-dimensional nanosheet structures in water. Compared to the individual monomers NA-TPA and MV-TPA, the SOF enhances electron transfer and significantly improves the generation of superoxide anion radicals ($O_2^{\bullet-}$), which in turn effectively promotes the photocatalytic cyclization reaction between *o*-phenylenediamine and benzaldehyde in water, achieving a yield of up to 94%. This work offers valuable insights into the design and construction of three-component SOFs based on encapsulation-enhanced donor-acceptor interactions for photocatalytic applications.

© 2026 Published by Elsevier B.V. on behalf of Chinese Chemical Society and Institute of Materia Medica, Chinese Academy of Medical Sciences.

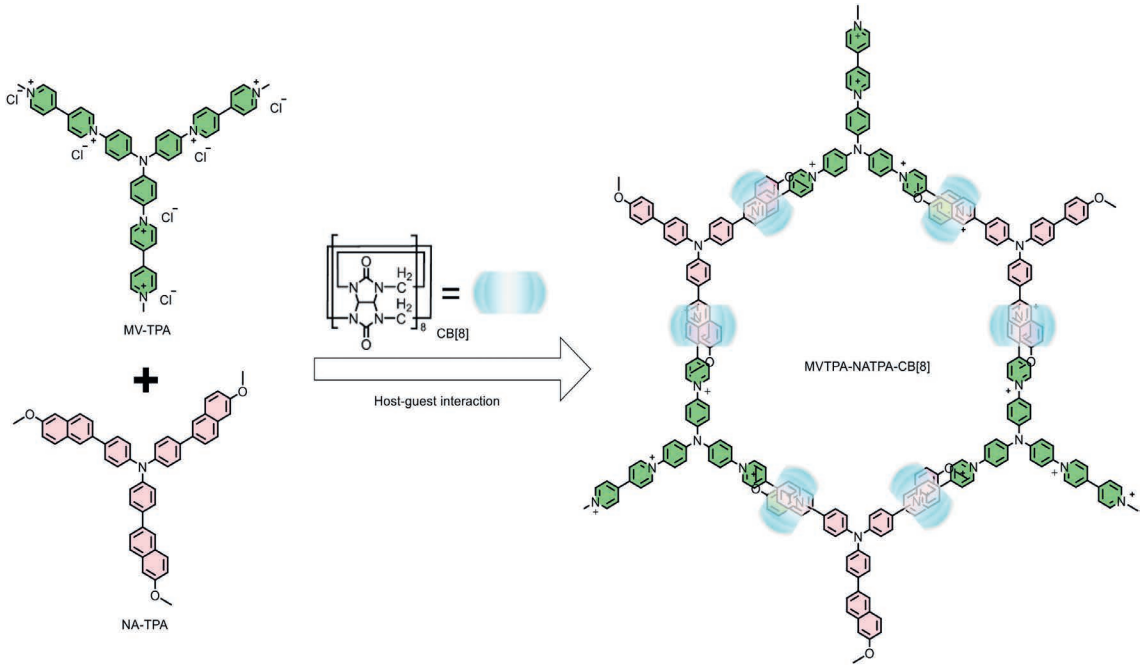
Supramolecular organic frameworks (SOFs) are a new kind of porous material that are made by self-assembly of noncovalent bonds [1–8]. They have quickly gained popularity in the field of materials science and have become a major focus of research in recent years [1–8]. These materials can create two-dimensional network architectures that are highly organized and functional by means of precise interactions between organic molecules, such as hydrogen bonding, π-π stacking, and metal ligand coordination [1–8]. SOFs not only have a high porosity and a large specific surface area, but they also have great stability and a variety of functional capabilities. These characteristics give them a wide range of possible applications in the domains of gas adsorption and separation [9–13], sensing [14–18], drug delivery [19,20], therapy [21,22], and catalysis [23–25].

With the continuous development of molecular self-assembly chemistry, the synthesis methods and performance control methods of SOFs are also constantly improved. Compared with traditional metal organic frameworks (MOFs) and covalent organic frameworks (COFs), SOFs have more flexible structural design and functionalization strategies. Their adjustable porosity, excellent specific surface area and good light absorption properties make them ideal photocatalyst carriers or directly used as photocatalytic materials in the fields of energy conversion and environmental governance [26–30]. The photocatalytic properties of SOFs are often closely related to their electronic structures. Due to its flexible molecular design, SOFs can enhance their absorption of visible or ultraviolet light by introducing organic dyes or conjugated structural units with good light absorption properties [31,32]. In addition, the interaction between organic molecules in SOFs helps to promote the transfer of electrons, improve the separation efficiency of photogenerated electron hole pairs, and further improve their catalytic activity [33–37].

In order to further explore the application of SOFs in photocatalytic organic conversion, we designed and synthesized a trimethoxynaphthyl-modified triphenylamine (NA-TPA) as the donor component, and a trimethylated viologen-modified triphenylamine (MV-TPA) as the acceptor component. Through the encapsulation-enhanced donor-acceptor interaction between methoxynaphthalene on NA-TPA and methylated viologen on MV-TPA, we constructed a novel donor-acceptor SOF with two-dimensional nanosheet morphology and uniform solubility in water. MVTPA-NATPA-CB[8] not only shows excellent superoxide an-

* Corresponding authors.
E-mail addresses: n.han@utoronto.ca (N. Han), lbxing@sdut.edu.cn (L. Xing).

https://doi.org/10.1016/j.cclet.2025.111426
1001-8417/© 2026 Published by Elsevier B.V. on behalf of Chinese Chemical Society and Institute of Materia Medica, Chinese Academy of Medical Sciences.



Scheme 1. Illustration of the construction of MVTPA-NATPA-CB[8] based on MV-TPA, NA-TPA and CB[8].

ion radicals ($O_2^{\bullet-}$) generation ability, but also can be used as a photocatalyst to achieve the synthesis of benzimidazole with a high yield of 94 % and a wide range of substrates (Scheme 1).

MV-TPA is synthesized through a one-step Zinke reaction followed by methylation (Scheme S1 in Supporting information), whereas NA-TPA is produced *via* a one-step Suzuki coupling reaction (Scheme S2 in Supporting information), which can be confirmed by ^{1}H NMR analysis (Figs. S1-S3 in Supporting information). To achieve effective water solubility for the self-assembly of MV-TPA in an aqueous solution containing NA-TPA and cucurbit[8]uril (CB[8]), we began by examining the UV–vis absorption and fluorescence emission spectra of the system. As shown in Fig. 1a, the absorption spectrum of the NA-TPA solution displays an absorption band between 250 nm and 280 nm, while MV-TPA exhibits two absorption bands in 250–320 nm and 350–550 nm. When NA-TPA and CB[8] were added to the MV-TPA solution in a 1:1:3 molar ratio, a significant increase in absorption was observed in the 370–600 nm region, along with a slight red shift. This suggests that the methoxynaphthyl group of NA-TPA and the methylated viologen group of MV-TPA were encapsulated within the CB[8] cavity, leading to enhanced donor-acceptor interactions. As shown in the fluorescence emission spectra of Fig. 1b, MV-TPA exhibited minimal fluorescence emission, while NA-TPA emitted strongly in the 350–450 nm range. The MVTPA-NATPA-CB[8] assembly (1:1:3 molar ratio) displayed decreased fluorescence emission in 350–450 nm range, which is lower than that of NA-TPA. This decrease in fluorescence emission is attributed to the inclusion of CB[8], which facilitates charge transfer between the electron-rich methoxynaphthyl and electron-deficient viologen units inside the CB[8] cavity. Fluorescence lifetime measurements (Fig. 1g) revealed values of 6.75 ns for MV-TPA, 9.12 ns for NA-TPA, and 4.58 ns for the MVTPA-NATPA-CB[8] complex.

The assembly structure of MVTPA-NATPA-CB[8] was further analyzed using dynamic light scattering (DLS) and zeta potential measurements. The hydrodynamic diameter (D_H) of the mixed aqueous solution was approximately 1200 nm, indicating the presence of large aggregates (Fig. 1c). Transmission electron microscopy (TEM) images revealed a uniform arrangement of two-dimensional nanosheets, providing strong evidence for the formation of SOF (Fig. 1e). Zeta potential measurements showed values of +2.18 mV for MV-TPA, −28.8 mV for NA-TPA, and +10.9 mV for the MVTPA-NATPA-CB[8] assembly (Fig. 1d), suggesting successful assembly through host-guest interactions between the components. Small-angle X-ray scattering (SAXS) analysis of the dried solid MVTPA-NATPA-CB[8] revealed a clear scattering peak with a D-spacing of 3.88 nm, confirming the periodic crystalline structure of the assembly (Fig. 1f). Additionally, ^{1}H NMR titration experiments (Fig. S4 in Supporting information) showed a significant decrease in the MV-TPA signal upon the addition of CB[8], likely due to the shielding effect of the CB[8] cavity. Chemical shifts of H1-H4 to lower field and a shift of the CB[8] characteristic peak further supported the encapsulation of the viologen unit of MV-TPA within the CB[8] cavity, providing additional evidence for the host-guest interaction driving the assembly of MVTPA-NATPA-CB[8].

Triphenylamine (TPA), a photosensitive building block, exhibits strong light absorption and efficient energy transfer properties [38]. To explore the potential applications of MVTPA-NATPA-CB[8], we investigated its ability to enhance photocatalytic oxidation processes. Specifically, we tested its capacity to generate singlet oxygen ($^1O_2$) using 9,10-anthracenediyl-bis(methylene)dimalonic acid (ABDA) as a probe. As shown in Fig. 1h and Fig. S5 (Supporting information), the addition of MV-TPA to the ABDA solution resulted in a significant decrease in ABDA absorption under blue light, indicating that MV-TPA efficiently produces $^1O_2$. In contrast, NA-TPA exhibited a weaker ability to generate $^1O_2$. Upon forming the MVTPA-NATPA-CB[8] complex, the $^1O_2$ production capacity was reduced. We further evaluated the production of superoxide anion radical ($O_2^{\bullet-}$) using tetramethylphenylenediamine (TMPD) as a probe. As shown in Fig. 1i and Fig. S5, solutions of MV-TPA and NA-TPA showed only weak absorption peaks at 563 nm and 612 nm when interacting with TMPD. In contrast, the MVTPA-NATPA-CB[8] complex exhibited distinct absorption peaks at both wavelengths, indicating a significantly higher capacity to generate $O_2^{\bullet-}$ compared to the individual components.

It is well known that the use of $O_2^{\bullet-}$ as the active substance to achieve oxidative cyclization of *o*-phenylenediamines and aromatic

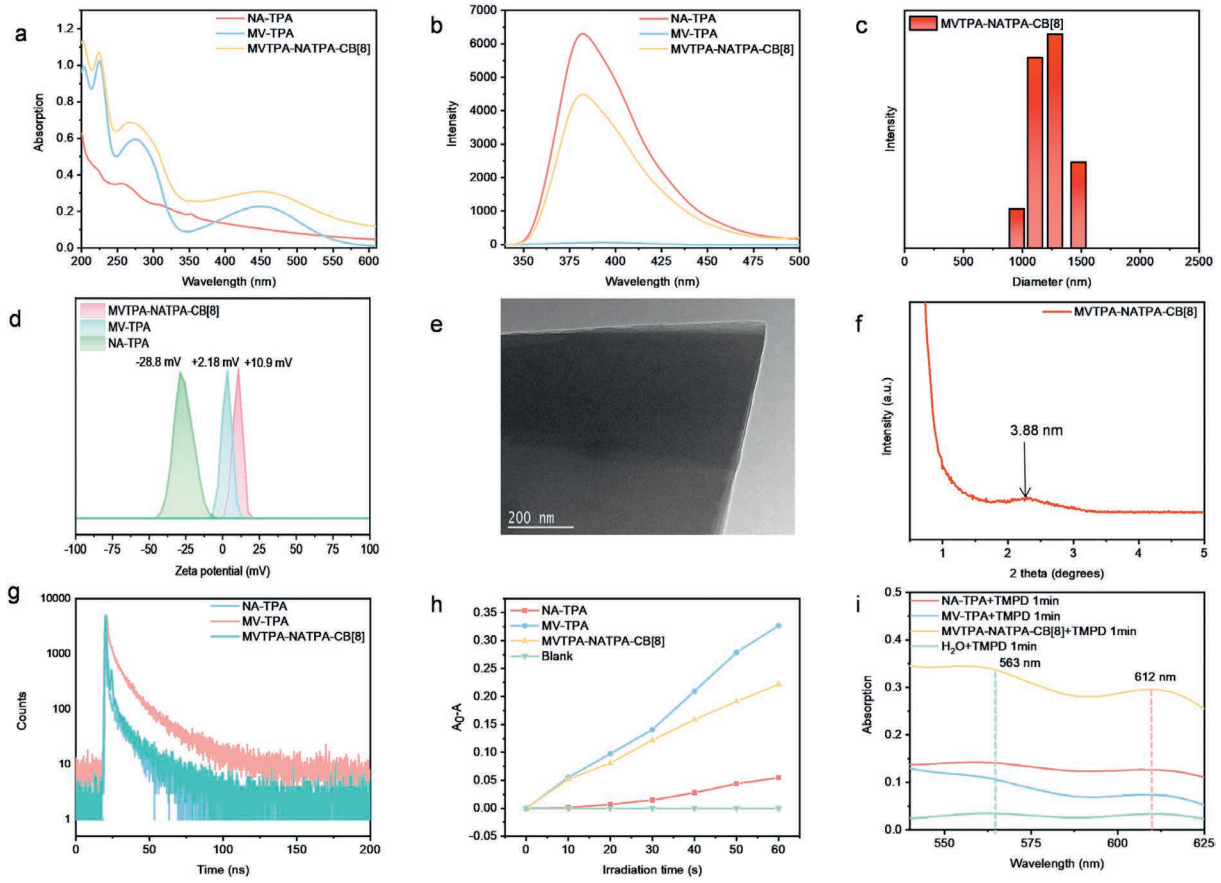


Fig. 1. (a) UV–vis absorption spectra and (b) fluorescence emission spectra of NA-TPA (2.0×10^{-5} mol/L), MV-TPA (2.0×10^{-5} mol/L), and MVTPA-NATPA-CB[8] (2.0×10^{-5} mol/L) in the aqueous solution. (c) DLS result of MVTPA-NATPA-CB[8] (2.0×10^{-5} mol/L). (d) Zeta potential of NA-TPA (2.0×10^{-5} mol/L), MV-TPA (2.0×10^{-5} mol/L), and MVTPA-NATPA-CB[8] (2.0×10^{-5} mol/L). (e) TEM image of MVTPA-NATPA-CB[8]. (f) Solid-phase SAXS profile of MVTPA-NATPA-CB[8]. (g) Time-resolved fluorescence decay curves of MV-TPA (2.0×10^{-5} mol/L), NA-TPA (2.0×10^{-5} mol/L) and MVTPA-NATPA-CB[8] (2.0×10^{-5} mol/L). (h) Normalized absorption quenching percentage of ABDA (1.0×10^{-4} mol/L) at 450 nm in the presence of MV-TPA (2.0×10^{-5} mol/L), NA-TPA (2.0×10^{-5} mol/L), and MVTPA-NATPA-CB[8] (2.0×10^{-5} mol/L) under blue light irradiation, blank: ABDA without any additives. (i) UV–vis absorption spectra of TMPD (1.0×10^{-4} mol/L) cationic radicals generated in the presence of MV-TPA (2.0×10^{-5} mol/L), NA-TPA (2.0×10^{-5} mol/L), and MVTPA-NATPA-CB[8] (2.0×10^{-5} mol/L), blank: TMPD without any additives.

Table 1
Optimization of the reaction conditions.[a]

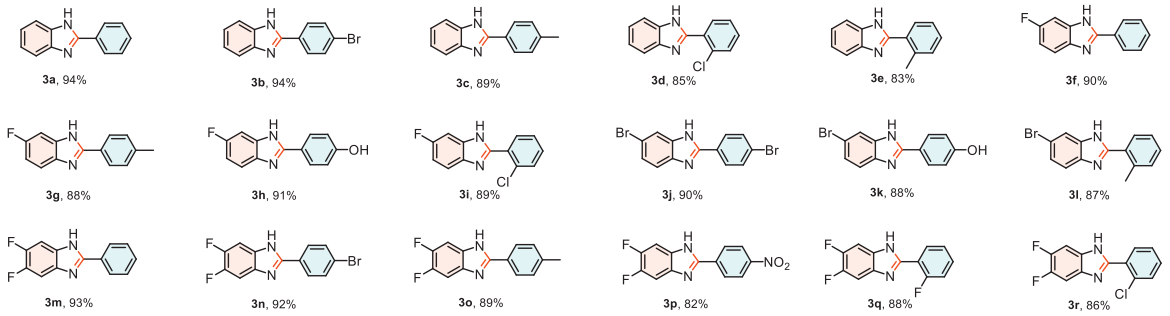


Entry	Variation from standard conditions	Yield (%)[b]
1	None	94
2	CB[8] instead of SOF	0
3	MV-TPA instead of SOF	32
4	NA-TPA instead of SOF	18
5	0.2 mol% instead of 0.5 mol%	47
6	1 mol% instead of 0.5 mol%	95
7	6 h instead of 12 h	64
8	18 h instead of 12 h	96
9	Without MVTPA-NATPA-CB[8]	No reaction
10	Without light	No reaction

[a] Standard conditions: *o*-phenylenediamine (0.1 mmol), benzaldehyde (0.1 mmol), H_2O (3.0 mL), blue LED (440–450 nm), air, room temperature, 12 h.
[b] Isolated yield.

aldehydes under visible light and the mild synthesis of benzimidazole are important strategies for forming key scaffolds in organic chemistry. As shown in Table 1, the experiment was carried out in ambient conditions for a duration of 12 h, using a blue LED as the source of excitation by using *o*-phenylenediamine and benzaldehyde as model substrates. The addition of 0.5 mol% MVTPA-NATPA-CB[8] to the system resulted in a high reaction yield of 94% (entry 1). In contrast, when CB[8], MV-TPA, or NA-TPA were used as catalysts individually, the yields were 0 (entry 2), 32% (entry 3), and 18% (entry 4), respectively. These results clearly show that MVTPA-NATPA-CB[8] significantly enhances the photocatalytic cyclization reaction between *o*-phenylenediamine and benzaldehyde. Reducing the photocatalyst concentration to 0.2 mol% led to a decreased yield of 47% (entry 5), while increasing the concentration to 1 mol% slightly improved the yield to 95% (entry 6). When the reaction time was shortened to 6 h, the yield dropped to 64% (entry 7), but extending the time to 18 h increased the yield to 96% (entry 8). Notably, when no photocatalyst was used (entry 9), no reaction occurred, highlighting the significant role of MVTPA-NATPA-CB[8] in enhancing the photooxidation process. Additionally, when the reaction was conducted in the absence of light (entry 10), no reaction occurred, confirming that light is essential for the process.

To assess the broader impact of MVTPA-NATPA-CB[8] on photooxidation processes, several *o*-phenylenediamine and aldehyde derivatives were subjected to photooxidation under the same lighting conditions. As shown in Scheme 2, when 0.5 mol% MVTPA-NATPA-CB[8] was used with blue light, the reaction proceeded efficiently with various *o*-phenylenediamine derivatives containing electron-withdrawing groups (-F, -Br) and aldehyde derivatives with both electron-withdrawing groups (-F, -Cl, -Br, $-NO_2$) and electron-donating groups ($-CH_3$, -OH,). High yields were achieved for reactions involving different derivatives, including 94% (**3a**),



Scheme 2. Substrates scope for the photocatalytic synthesis of benzimidazole by MVTPA-NATPA-CB[8].

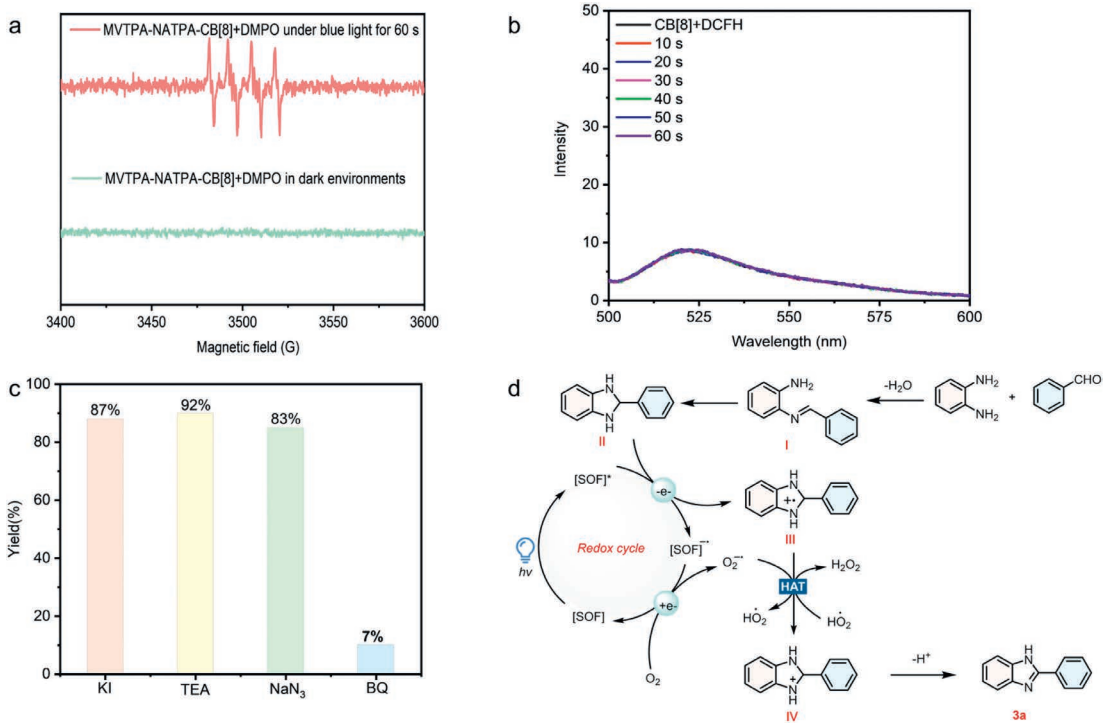


Fig. 2. (a) EPR measurement of MVTPA-NATPA-CB[8] (2.0×10^{-5} mol/L) in the presence of DMPO under blue light for 60 s and under dark environments. (b) Fluorescence emission spectra of CB[8] in the presence of DCFH under the blue light irradiation. (c) Control experiments. (d) Proposed mechanism.

94% (**3b**), 89% (**3c**), 85% (**3d**), 83% (**3e**), 90% (**3f**), 88% (**3 g**), 91% (**3h**), 89% (**3i**), 90% (**3j**), 88% (**3k**), 87% (**3l**), 93% (**3m**), 92% (**3n**), 89% (**3o**), 82% (**3p**), 88% (**3q**), and 86% (**3r**). These results confirm that MVTPA-NATPA-CB[8] is highly effective for generating benzimidazole derivatives through photooxidative coupling reactions involving various *o*-phenylenediamine and aldehyde derivatives.

Electron paramagnetic resonance (EPR) spectroscopy was used to detect the generation of reactive oxygen species (ROS), with 5,5-dimethyl-1-pyrroline-*N*-oxide (DMPO) as a scavenger for $O_2^{\bullet-}$. No ROS signal was observed in the MVTPA-NATPA-CB[8] solution when DMPO was added before irradiation (Fig. 2a). However, upon excitation with blue light, an $O_2^{\bullet-}$ signal was detected. To assess the effect of CB[8] on ROS generation, 2′,7′-dichlorodihydrofluorescein (DCFH) was used as a fluorescence-based detection reagent. As shown in Fig. 2b, the introduction of DCFH into the CB[8] solution under light exposure did not result in any significant change in the fluorescence emission spectra. This observation suggests that CB[8] lacks the capacity to produce ROS.

In the photocatalytic cyclization reaction between *o*-phenylenediamine and benzaldehyde, early investigations have demonstrated the significant involvement of $O_2^{\bullet-}$ [39–41]. Hence, to examine the reaction mechanism, we incorporated many active species scavengers in the comparative analysis of the photocatalytic cross coupling reaction involving aromatic diamine and aromatic aldehyde. Fig. 2c illustrates that the use of KI as a hole scavenger, triethylamine (TEA) as a hydroxyl radical ($^{\bullet}OH$) scavenger, and NaN_3 as a scavenger of $^1O_2$ did not result in any significant changes in the yields. This finding indicates that the existence of holes, $^{\bullet}OH$, and $^1O_2$ did not have any noticeable impact on the photocatalytic process. However, the incorporation of *p*-benzoquinone (BQ), which functions as a scavenger for $O_2^{\bullet-}$, led to a significant decrease (7%) in the conversion efficiency. This finding offers validation for the concept that $O_2^{\bullet-}$ is the main active species participating in the photoredox coupling reaction of *o*-phenylenediamine and benzaldehyde. Fig. 2d shows the proposed photocatalytic mechanism based on previous research. Exposure to blue light induces the catalyst [SOF] to transform into its excited state [SOF]*. Subsequently, the cyclization intermediate **II** of imine **I** acts as an electron donor for [SOF]*, producing $[SOF]^{\bullet-}$ and intermediate **III**. In addition, the direct electron transfer be-

tween $[SOF]^{\bullet-}$ and triplet oxygen ($^3O_2$) leads to the production of $O_2^{\bullet-}$, which subsequently returns to the ground state [SOF]. In addition, $O_2^{\bullet-}$ can act as a hydrogen atom transfer (HAT) agent, and intermediate **III** will undergo additional reactions with $O_2^{\bullet-}$ through the HAT mechanism, forming $HO_2^{\bullet}$ and intermediate **IV**, ultimately converting into final product **3a** and H_2O_2.

In summary, we have developed two photosensitive modules, utilizing NA-TPA as the donor unit and MV-TPA as the acceptor unit. These modules form a novel two-dimensional SOF in aqueous solution through encapsulation-enhanced donor-acceptor interactions with CB[8], leading to the spontaneous formation of two-dimensional nanosheet structures. The resulting SOF exhibits excellent electron transfer capabilities, significantly boosting the production of superoxide anion radicals ($O_2^{\bullet-}$), which in turn enhances the photocatalytic cyclization reaction between *o*-phenylenediamine and benzaldehyde in water, achieving yields of up to 94%. This study introduces a new approach for constructing three-component SOFs based on encapsulation-enhanced donor-acceptor interactions and ROS enhancement, and demonstrates their effective application in photocatalytic organic conversions.

Declaration of competing interest

The authors declare that they have no known competing financial interests or personal relationships that could have appeared to influence the work reported in this paper.

CRediT authorship contribution statement

Xianya Yao: Writing – original draft, Investigation, Formal analysis, Data curation. **Ning Han:** Writing – review & editing, Supervision, Conceptualization. **Hui Liu:** Writing – review & editing, Formal analysis, Data curation, Conceptualization. **Lingbao Xing:** Writing – review & editing, Investigation, Funding acquisition, Formal analysis, Data curation, Conceptualization.

Acknowledgments

We are grateful for the financial support from the National Natural Science Foundation of China (No. 52205210) and the Natural Science Foundation of Shandong Province (No. ZR2022QE033).

Supplementary materials

Supplementary material associated with this article can be found, in the online version, at doi:10.1016/j.cclet.2025.111426.

References

[1] K.D. Zhang, J. Tian, D. Hanifi, et al., J. Am. Chem. Soc. 135 (2013) 17913–17918.
[2] Z.T. Li, S.B. Yu, Y. Liu, et al., Acc. Chem. Res. 55 (2022) 2316–2325.
[3] J. Tian, F. Lin, S.B. Yu, et al., Aggregate 3 (2022) e187.
[4] J. Tian, L. Chen, D.W. Zhang, et al., Chem. Commun. 52 (2016) 6351–6362.
[5] S.B. Yu, F. Lin, J. Tian, et al., Chem. Soc. Rev. 51 (2022) 434–449.
[6] M.N. Shen, X.W. Lin, J. Luo, et al., Mol. Syst. Des. Eng. 7 (2022) 1570–1587.
[7] J. Tian, H. Wang, D.W. Zhang, et al., Natl. Sci. Rev. 4 (2017) 426–436.
[8] S.Y. Jiang, X. Zhao, Chin. J. Polym. Sci. 37 (2018) 1–10.
[9] J. Tian, T.Y. Zhou, S.C. Zhang, et al., Nat. Commun. 5 (2014) 5574.
[10] A. Chaix, G. Mouchaham, A. Shkurenko, et al., J. Am. Chem. Soc. 140 (2018) 14571–14575.
[11] W. Yang, A. Greenaway, X. Lin, et al., J. Am. Chem. Soc. 132 (2010) 14457–14469.
[12] J. Lu, C. Perez-Krap, M. Suyetin, et al., J. Am. Chem. Soc. 136 (2014) 12828–12831.
[13] L.L. Tan, H. Li, Y. Tao, et al., Adv. Mater. 26 (2014) 7027–7031.
[14] C. Yan, Q. Li, X. Miao, et al., Angew. Chem. Int. Ed. 62 (2023) e202308029.
[15] Y. Li, Q. Li, X. Miao, et al., Angew. Chem. Int. Ed. 60 (2021) 6744–6751.
[16] Y.Q. Yao, Y.J. Zhang, C. Huang, et al., Chem. Mater. 29 (2017) 5468–5472.
[17] J. Liu, Y.Q. Fan, S.S. Song, et al., ACS Sustain. Chem. Eng. 7 (2019) 11999–12007.
[18] Y. Zhang, T.G. Zhan, T.Y. Zhou, et al., Chem. Commun. 52 (2016) 7588–7591.
[19] C. Yao, J. Tian, H. Wang, et al., Chin. Chem. Lett. 28 (2017) 893–899.
[20] J.L. Lin, Z.K. Wang, Z.Y. Xu, et al., J. Am. Chem. Soc. 142 (2020) 3577–3582.
[21] W. Wang, B. Qi, X. Yu, et al., Adv. Funct. Mater. 30 (2020) 2004452.
[22] Z.Y. Xu, W. Mao, Z. Zhao, et al., J. Mater. Chem. B 10 (2022) 899–908.
[23] J. Tian, Z.Y. Xu, D.W. Zhang, et al., Nat. Commun. 7 (2016) 11580.
[24] X.F. Li, S.B. Yu, B. Yang, et al., Sci. China Chem. 61 (2018) 830–835.
[25] H.J. Lee, H.J. Kim, E.C. Lee, et al., Chem. Asian J. 13 (2018) 390–394.
[26] W. Xu, J.Y. Chao, B. Tang, et al., Chem. Eur. J. 28 (2022) e202202200.
[27] Y. Fan, Y. Luo, X. Luo, et al., Green Chem. 26 (2024) 12076–12083.
[28] Y. Fan, J. Tan, C. Zou, et al., Chin. Chem. Lett. 36 (2025) 110101.
[29] H. Du, M. Zhao, X. Lang, et al., Chem. Commun. 60 (2024) 7598–7601.
[30] Y.P. Wu, M. Yan, Z.Z. Gao, et al., Chin. Chem. Lett. 30 (2019) 1383–1386.
[31] D. Ren, L. Tang, Z. Wu, et al., Chin. Chem. Lett. 34 (2023) 108617.
[32] H. Qian, T. Xiao, R. Elmes, et al., Chin. Chem. Lett. 34 (2023) 108185.
[33] X.Y. Yao, S. Yu, R.Z. Zhang, et al., Sci. China Mater. 67 (2024) 833–841.
[34] X.Z. Yang, R.X. Zhu, R.Y. Zhu, et al., J. Colloid Interface Sci. 658 (2024) 392–400.
[35] F.D. Wang, K.K. Niu, X.Y. Yao, et al., J. Mater. Chem. A 12 (2024) 16190–16199.
[36] M. Jiang, Y. Wang, H. Liu, et al., J. Mater. Chem. A 12 (2024) 4752–4760.
[37] Y. Wang, C.Q. Ma, X.L. Li, et al., J. Mater. Chem. A 11 (2023) 2627–2633.
[38] T. Xiao, X. Li, L. Zhang, et al., Chin. Chem. Lett. 35 (2024) 108618.
[39] A. Dewanji, L. van Dalsen, J.A. Rossi-Ashton, et al., Nat. Chem. 15 (2023) 43–52.
[40] X. Wu, A.P. Davis, A.J. Fry, Org. Lett. 9 (2007) 5633–5636.
[41] Z. Li, H. Song, R. Guo, et al., Green Chem. 21 (2019) 3602–3605.